Arch. Metall. Mater. **69** (2024), 3, 1061-1069

DOI: https://doi.org/10.24425/amm.2024.150926

S. BOCZKAL[1], M. WĘGRZYN[1], W. SZYMAŃSKI[1], J. BEM[1], K. WALA[1], B. PŁONKA[1], D. LEŚNIAK[2], M. NOWAK[1]

EFFECT OF AGING PARAMETERS OF EN AW-7021 ALUMINIUM ALLOYS ON STRESS CORROSION CRACKING

The main assumption of the conducted research was the selection of appropriate heat treatment parameters to obtain the best possible resistance to stress corrosion cracking (SCC) and the highest strength properties of the extruded profiles. The work selected the temperature and time of one- and two-stage treatment of the EN AW-7021 alloy based on aging curves. Tests carried out for samples after aging at 135°C for 24 h and two-stage aging at 90°C/8 h + 135°C/8 h revealed the highest resistance to SCC. The 7021 alloy, after heat treatment at 90°C/8 h + 135°C/16 h, reached the highest tensile strength of 534MPa. Transmission electron microscopy (TEM) observations showed slight differences in the finely dispersed nucleoids between the selected parameters of the artificial aging process.

Keywords: Extruded elements; High-strength aluminium; Heat treatment; Stress corrosion cracking

1. Introduction

The aluminum alloys of the 7XXX series (Al 7XXX alloys) are widely used in structural elements, in the aerospace and automotive industries, due to their high strength, high specific stiffness, excellent machining and weldability [1]. These alloys whose properties can be adjusted in a wide range and adapted to a given application because of the possibility of precipitation strengthening by appropriate heat treatment. After supersaturation of the Al-Zn-Mg alloy, the solid solution decomposes first into Guinier-Preston (GP) zones, then into unstable η' precipitates to finally form the η equilibrium phase during aging [2,3]. However, this strengthening mechanism increases the susceptibility of the alloy to SCC.

Traditional 7xxx series aluminum alloy has the highest strength at the peak of the aging curve (T6), but its SCC resistance is low. There are several types of heat treatment, such as over aging, two-stage aging or regression re-aging (RRA), which can significantly improve the corrosion resistance of the alloy, and the loss of strength is relatively small [4]. In alloys of the 7xxx series, heat treatment is carried out at relatively low temperatures and short times, which affects the maintenance of a high level of strengthening over time. Increasing the temperature results in a rapid decomposition of the solid solution and a rapid decrease in strengthening. During two or more stages of aging, finely dispersed η' phases appear. During the transition from a lower temperature to a higher temperature, the η' phase grows and is transformed into the η phase. Grain boundary phases can also be observed [4].

Minimal changes in the Zn/Mg ratio and alloy additives in the 7xxx series alloys make it necessary to reselect heat treatment conditions in order to block the phenomenon of crack propagation during SCC tests [5].

The SCC phenomenon occurs when a material is stressed in an aggressive environment. It causes degradation of the material at the level of stresses lower than the strength values of the material, in ambient conditions where corrosion itself may not necessarily lead to damage. Crack initiation and propagation observed during SCC occurs in many metals and alloys, including the 7xxx series alloys. These materials, usually due to their high strength, are widely used as lightweight load-bearing structures; therefore, it is necessary to know about the progress of crack propagation under stress in an aggressive environment [6-8].

The tests carried out show that the 7xxx series alloys are resistant to SCC when the Zn/Mg ratio is low, Zr or Sc is used as a microaddition to the alloys, and when a two- or more-stage heat treatment is performed [9].

As part of the research work, new heat treatment parameters were selected for the variant of the EN AW-7021 alloy. The developed heat treatment parameters were to ensure the assumed levels of mechanical properties of extruded profiles in industrial conditions and, additionally, high resistance to SCC.

[1] ŁUKASIEWICZ RESEARCH NETWORK – INSTITUTE OF NON FERROUS METALS, LIGHT METALS CENTRE, 19 PILSUDKSIEGO STR., 32-050 SKAWINA, POLAND
[2] AGH UNIVERSITY OF KRAKÓW, FACULTY OF NON-FERROUS METALS, AL. MICKIEWICZA 30, 30-059 KRAKOW, POLAND

* Corresponding author:

The microstructure and mechanical properties of the alloy were characterised after various variants of artificial aging.

2. Materials and methods

2.1. Material information

The EN AW-7021 alloy was prepared from pure ingredients: aluminium billets melted in a furnace, then supplemented with alloy components. Casting was carried out on a semi-continuous, vertical casting station using a Hot-Top crystallizer with a diameter of 254 mm and 2000 mm long (Fig. 1a). The chemical composition of the alloy tested analyzed with the ARL 4460 optical emission spectrometer is shown in TABLE 1.

TABLE 1

Chemical composition of billets of alloy EN AW-7021 [wt.%]

Fe	Si	Cu	Zn	Ti	Mn	Mg	Cr	Zr	Al
0,086	0,033	0,010	**5,46**	0,02	0,003	**2,12**	0,001	0,15	rest

The cast billets were homogenized by heating to a temperature of 465°C for 10 hours, heating for 4 hours and then quick cooling with the use of fans and then skinned to prepare them for extrusion. Extrusion was carried out at Albatros Aluminum on a 32 MN press with a 254 mm container in the temperature range of 460-500°C. Flat bars with dimensions of 62.3×3 mm were saturated on the press run with air blowing (Fig. 1b).

2.2. Aging heat treatment

Samples of about 300 mm in length were taken from the sections for further testing. To determine the aging curves, 10 samples with dimensions of 30×30 mm of each aging variant were prepared.

TABLE 2

Variants of artificial aging [°C]

One-stage		Two-stage	
A1	**A2**	**B1**	**B2**
135	160	90/8 h+135	90/8 h+160

According to the literature data [4,5,8-11], the two-stage heat treatment is selected due to the expected effect of increasing the density of the GP zone dispersion by extending the aging time at temperatures below their zone solubility, i.e. <150°C. This second stage leads to the multiplication in the number of particles of the reinforcement phase η' and thus may lead to an increase in strength and resistance to corrosion. Therefore, the

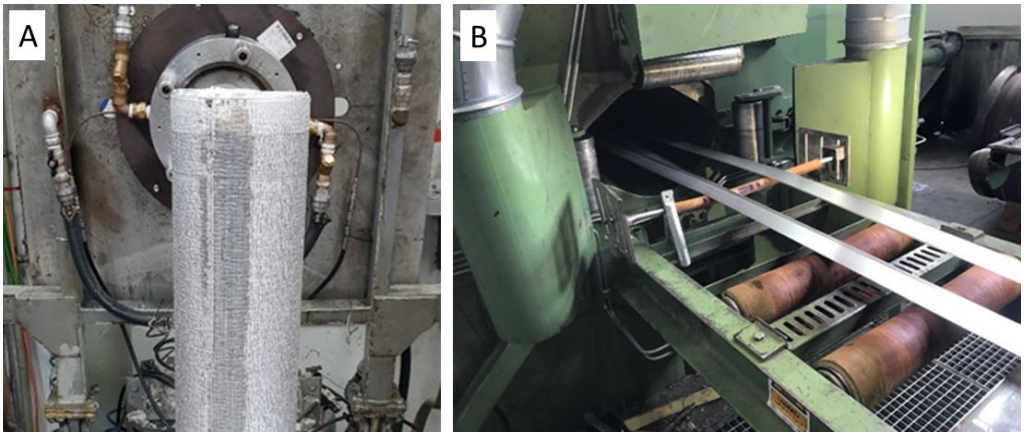

Fig. 1. a) cast 10” ingot with a casting table in Łukasiewicz-IMN, b) press overrun during industrial tests in Albatros Aluminum

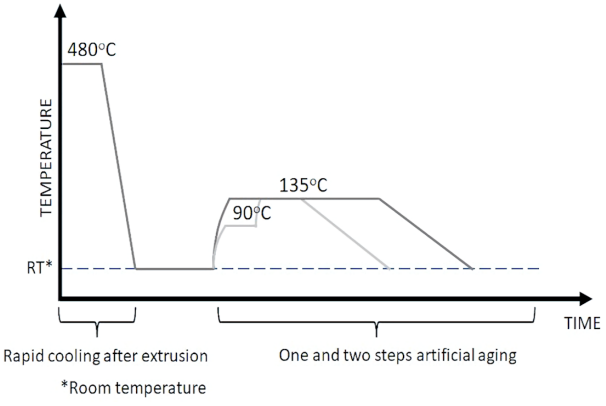

Fig. 2. Scheme of heat treatment

work proposed, 2 one- and 2 two-stage artificial aging temperatures were selected (TABLE 2). The aging was carried out in the LAC PP40/65 furnace. After removal from the oven, the samples were cooled in the air. The level of hardening in the aging process was tested by measuring the Brinell hardness on an automated Duramin 2500E hardness tester.

Samples were taken every 0.5 h, 1 h, 3 h, 6 h, 10 h, 16 h, 24 h, 36 h, 48 h, 72 h. On each of the 40 samples, 4 hardness imprints were made and the average was determined. The tests for 4 temperature variants were carried out until the hardness decreased. Then, based on the aging curves, 2 temperatures and 2 time variants were selected. Aging was carried out on samples 300 mm long according to the scheme shown in Fig. 2.

The time from extrusion and solution saturation on the press runway to aging did not exceed 6 h. Heat-treated samples were prepared for TEM microstructure and strength tests. Thin films were made from the samples by grinding and electropolishing of both sides on the TENUPOL device in Struers A2 reagent. Observations were carried out on a Tecnai G20 X-twin transmission electron microscope (TEM) with an FEI HAADF and EDS attachment. Selected area diffraction (SAD) analyses were performed using ICDD PDF 4+ software.

2.3. SCC test

The SCC test was performed according to the ECSS-Q-ST-70-37C standard [12]. This standard covers SCC testing of metal samples under constant load. According to the standard, properly prepared samples were exposed to a 3.5% NaCl solution for 10 minutes in an hour-long cycle. The test was carried out at a stress of 75% of the conventional stress YS. The samples were stressed with a force of 6 kN. The tests were carried out under alternating immersion conditions for a 30-day exposure period. One liter of the solution was provided for each pair of samples and replaced after seven, fourteen and 21 days. The unstressed control samples were exposed to the same environment to provide a basis for comparing in assessing the susceptibility to stress cracking of materials that survived the 30-day exposure period. Corrosion susceptibility was assessed using a static tensile test to compare the residual strength of exposed, stressed, and unstressed specimens. A static tensile test was carried out in accordance with the standard for a static tensile test [13] method B on an Instron 5582 (maximum load 100 kN) for samples before and after stress corrosion cracking. Metallographic microsections of longitudinal sections of strength samples were examined to classify susceptibility to SCC. Specimens for observation in the light microscope (LM) were prepared by grinding and mechanical polishing. Observations were carried out using a Zeiss Axio Observer 7 LM at magnifications of ×50 and ×500. The average grain size was measured using the secant method on 100 grains on a cross-section sampled from a flat bar. The grains were revealed by the Barker method.

3. Results

3.1. Material

Flat bars made of the EN AW-7021 alloy after the solution solution process on the run-out of the press were analyzed in terms of structure and properties. The average grain size was approx. 6.5 mm. The microstructure observed on TEM was characterized by elongated grains in the extrusion direction. The sub-grain structure dominated (Fig. 3), where apart from the boundaries of a large angle, dislocation boundaries running inside the grains were visible. The tested sample found no finely dispersed GP phases or η' phases.

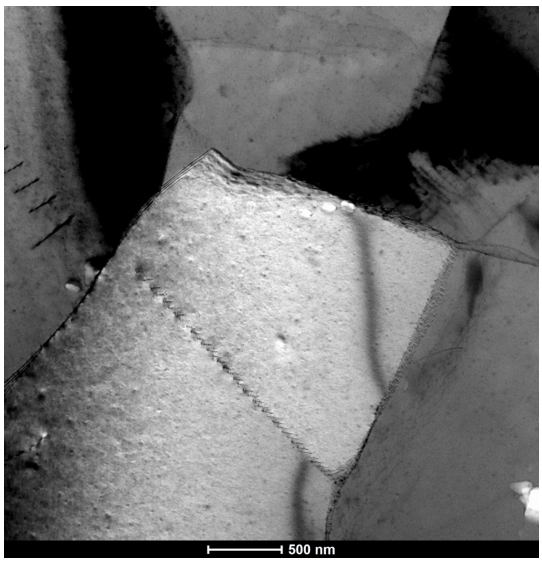

Fig. 3. BF of a flat bar sample after extrusion and solution on the runway of the press

Strength properties were at a low level, which confirms the unhardened state of the tested sample (TABLE 3). The tensile strength was about 380 MPa, the yield strength was about 240 MPa, and the elongation was 15%.

TABLE 3

Strength properties of the material after solution on the press

After extrusion			
Sample name	**YS [MPa]**	**UTS [MPa]**	**A [%]**
F	243±0,6	386 ±0,5	15,0 ±0,1

3.2. Artificial aging

Based on the aging curves (Fig. 4), four variants of heat treatment were selected, characterised by the highest and stabilised hardness. It was also observed that after 16h of aging at 135°C the samples did not reach the highest hardness, but the difference between the highest hardness and after 16 h was small and amounted to approx. 8HB. The hardness after 16 h for one-stage aging is approximately 149HB and for two-stage aging

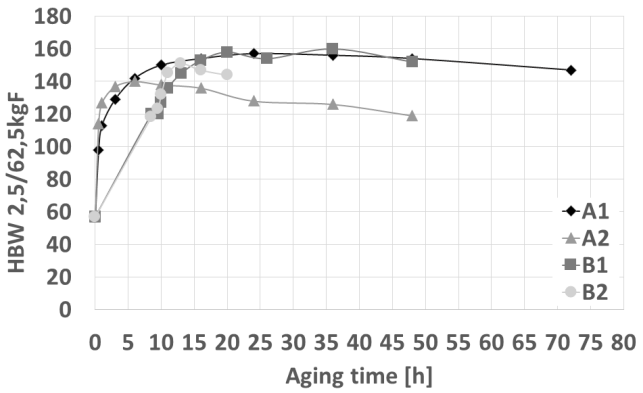

Fig. 4. Aging curves – Brinell hardness as a function of aging time

it is approximately 150HB. The highest hardness of the sample is reached after approx. 24 h. After this time, the strengthening curve slightly decreases. For this reason, the aging process was selected so that in both one- and two-stage aging, the material had the highest hardening, in the case of 16h with a rising trend, in the case of 24 h with a decreasing tendency on the hardening curve. The aim of these analyzes was the most optimal selection of aging process conditions in terms of strength properties and resistance to SCC. Then, one-stage aging at 135°C for 16 h (A1/16) and 24 h (A1/24) and two-stage aging at 90°C for 8 h + 135°C for 16 h (B1/16) and 24 h (B1/24) were carried out on the supplied flat bars.

TEM microstructure studies showed slight differences between the samples under selected aging conditions (Fig. 5). Finely dispersed η' phases were visible in all variants of the tested samples. After two-stage aging in sample B1/16, a higher density of fine-disperse phases was also observed (Fig. 5c) compared to the remaining samples. Based on the SAD analysis, Al_3Zr phases were found in this sample. Zr was present in the chemical composition of the alloy and in the form of Al_3Zr phases can be randomly distributed in the volume of the alloy. In samples after single-stage aging for 24 h (A1/24) and two-stage aging for 16 h (B1/16) and 24 h (B1/24), areas with clustered fine precipitates from the $MgZn_2$ phase with dimensions of approx. 70 nm were observed (Fig. 6).

Static tensile tests of samples taken from aged flat bars are shown in TABLE 4. After heat treatments in this artificial aging, 7021 alloys have a high tensile strength of >500 MPa. In the tested samples, after various aging variants, the property results remained at a similar level (TABLE 4). However, after carefully analysing the results, there were minor deviations. The highest tensile strength was found in sample B1/24 (534 MPa), while the lowest was shown in sample A1/16 (521 MPa). Samples A1/16,

TABLE 4

Strength properties of the material after artificial aging

Reference			
Sample name	**YS [MPa]**	**UTS [MPa]**	**A [%]**
A1/16	485±1,0	521±0,6	11,9±0,3
A1/24	488±0,6	524±1,2	11,9±0,5
B1/16	463±1,0	526±0,6	14,5±0,8
B1/24	486±0,6	534±2,0	13,3±0,5

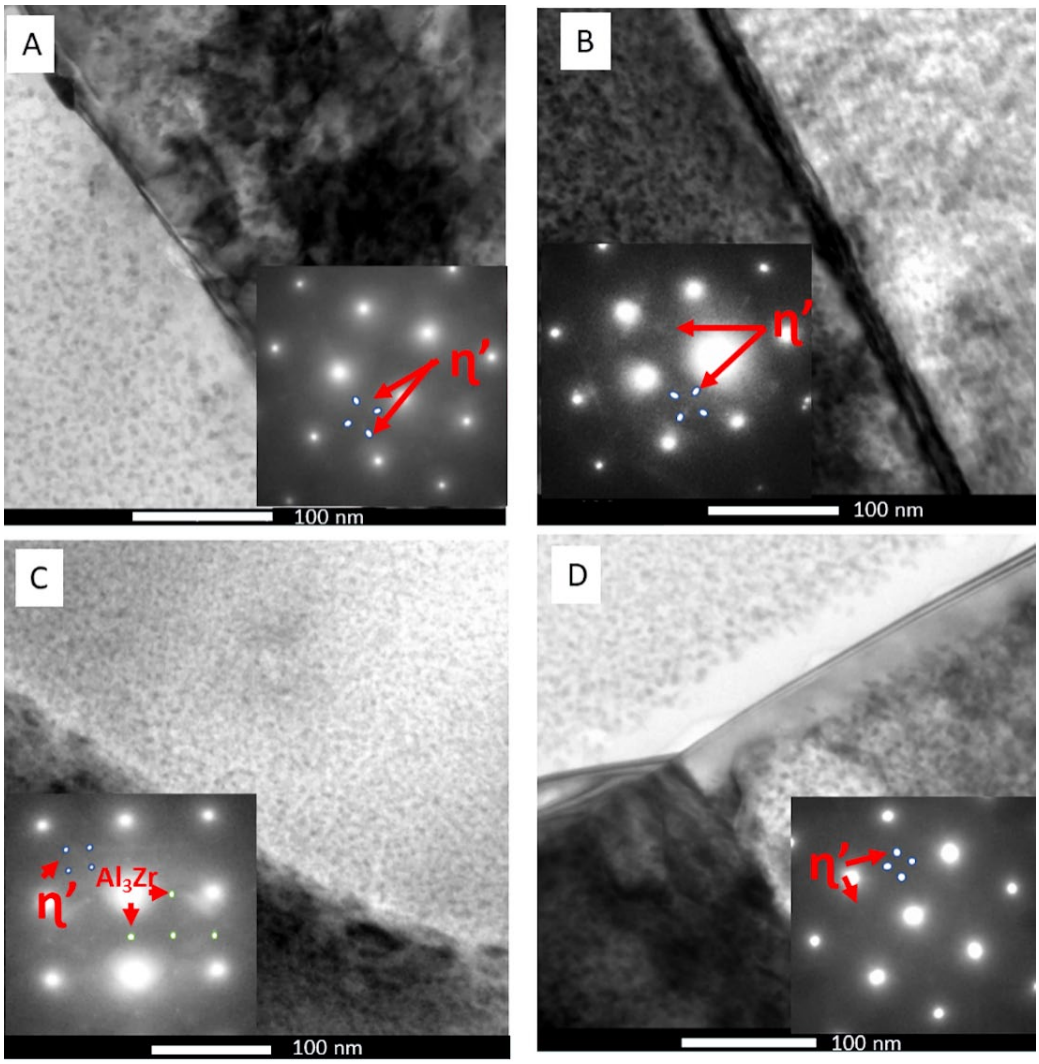

Fig. 5. Braight field (BF) image with SAD on (100) in samples after a) 135°C/16h, b) 135°C/24 h, c) 90°C/8 h + 135°C/16 h and d) 90°C/8 h + 135°C/24 h

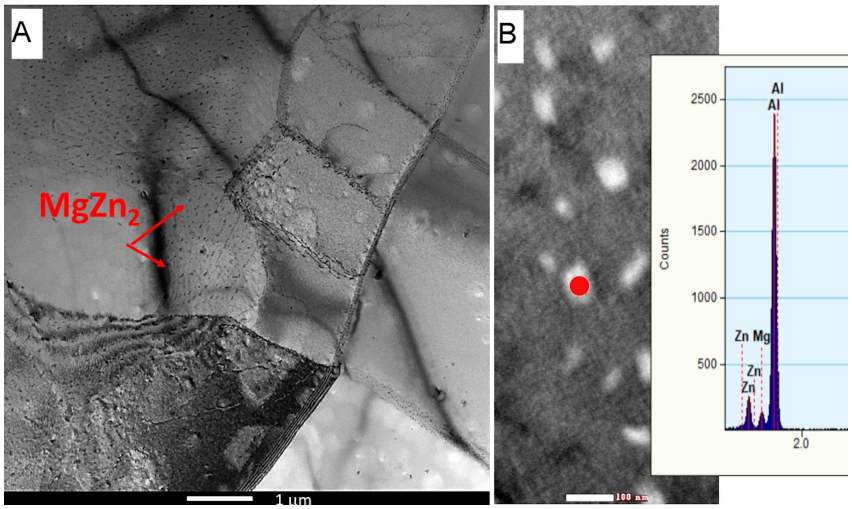

Fig. 6. Example of a) Bright field (BF) image and b) STEM with EDS point analysis in samples after 90°C/8 h + 135°C/24 h with non-homogeneously distributed areas of $MgZn_2$ precipitates

A1/24 and B1/16 showed comparable tensile strength results. The differences between them oscillated in the range of 5 MPa. In the B1/16 sample, the lowest yield strength (463 MPa) and the highest elongation of 14.5% were found. The remaining tested samples were characterised by a higher yield point and lower elongation. The elongation after one-stage aging was about 12%, and after two-stage aging in the B1/24 sample it was about 13%. All samples tested after artificial aging were characterised by about 1-3% lower elongation than the elongation of the sample in the F state (15%) (TABLE 3).

3.3. SCC

After the artificial aging process, flat bar samples were tested on specially designed SCC machines. The samples were tested under a load of 6 kN and without a load for 30 days. After a 30-day exposure in a 3.5% NaCl solution, the samples did not cracked, indicating a positive test result. In addition, to determine the degree of corrosion and stress corrosion, they were subjected to a static tensile test (Fig. 7, TABLE 4 and TABLE 5) and observations on the LM (Figs. 8 and 9).

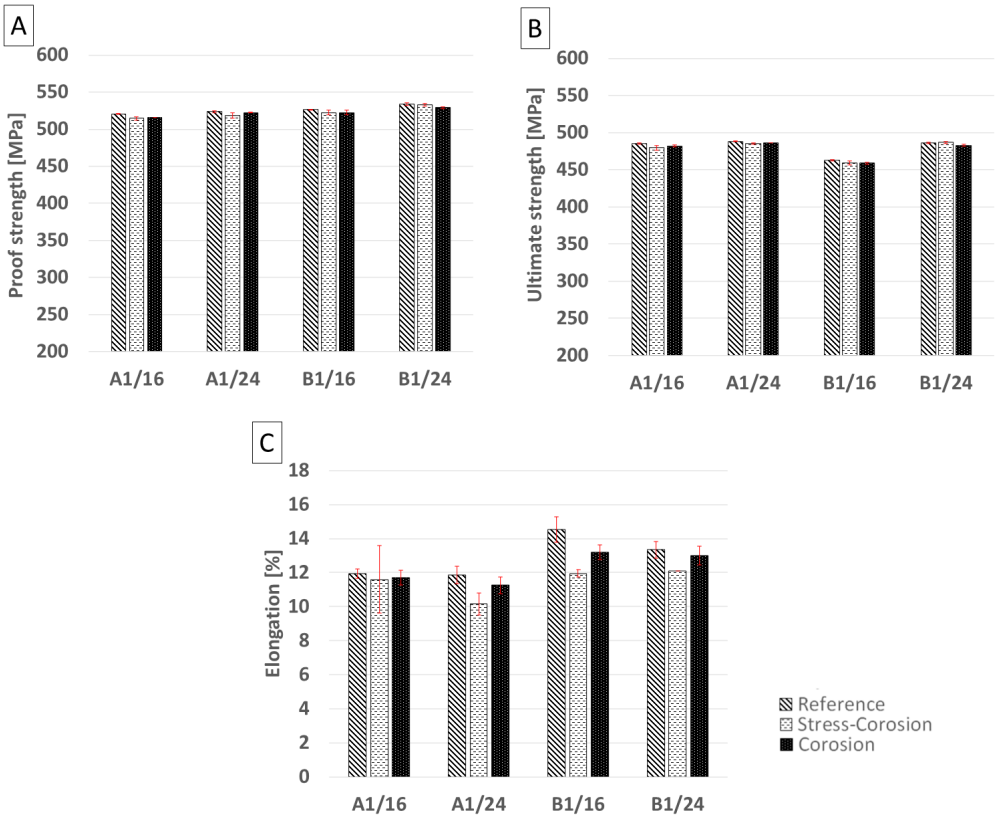

Fig. 7. Strength properties of the EN-AW 7021 aluminium alloy in reference state, under stress and corrosion agent and only under corrosion agent a) YS [MPa], b) UTS [MPa] and c) A [%] charts

Based on the diagrams of changes in yield strength (Fig. 7a) and tensile strength (Fig. 7b), no apparent differences were found between the reference samples and those subjected to corrosion and SCC. The sample after artificial aging B1/16 compared to the other samples was characterized by the lowest yield strength both before and after corrosion and stress corrosion tests. The tensile strength limit was comparable for all samples and amounted to approx. 520 MPa. No influence of corrosion tests on the strength limit was found.

Sample B1/16, compared to other samples with other artificial aging parameters, was characterized by the lowest yield strength and the highest percentage elongation (Fig. 7c). When analysing the percentage of elongation, a decrease from 0.5% to 3.1% was observed in all tested samples subjected to heat treatment compared to the sample from the initial state (TABLE 3 and TABLE 4) and a decrease in plasticity for samples subjected to SCC (Fig. 7c). The largest decrease of about 3% was found for the B1/16 sample compared to the others. After the corrosion test of the unstressed samples, a slight decrease in elongation was observed, not exceeding 2%.

Based on the observation of the microstructure of the LM samples subjected to corrosion and stress corrosion tests in 3.5% NaCl, pitting and intergranular corrosion were found. The microstructure was observed from the side of the longitudinal section of the sample. Three samples of each variant of artificial aging were subjected to post-corrosion and stress corrosion tests,

TABLE 5

Results of the strength properties with standard deviation of the EN-AW 7021 aluminium alloy after corrosion and SCC test

After stress – corrosion			
Sample name	**YS [MPa]**	**UTS [MPa]**	**A [%]**
A1/16	480±3,5	515±2,1	11,6±2,0
A1/24	486±0,7	519±3,5	10,2±0,6
B1/16	459±2,8	523±3,5	12,0±0,2
B1/24	487±1,4	533±1,4	12,1±0,0
After corrosion only			
Sample name	**YS [MPa]**	**UTS [MPa]**	**A [%]**
A1/16	482±1,4	516±0,0	11,7±0,4
A1/24	486±0,0	523±0,7	11,3±0,5
B1/16	459±1,4	523±3,5	13,2±0,4
B1/24	473±1,4	523±1,4	12,2±0,6

observing the upper and lower sections. First, the samples after SCC were analysed (Fig. 8). In samples A1/16 and B1/24 SCC was found at ×50 magnification (Fig. 8a, c). At ×500 magnification, the pits and the beginning of intergranular corrosion were clearly visible (Fig. 8b, d). The depth of the pit in the A1/16 sample was the largest and amounted to approximately 120 µm, and in the B1/24 sample it was approximately 60 µm.

After corrosion, similarly to SCC, all samples were analysed. Pitting was observed on four aged specimens A1/16, A1/24, B1/16 and B1/24. Due to their shape, the pits visible

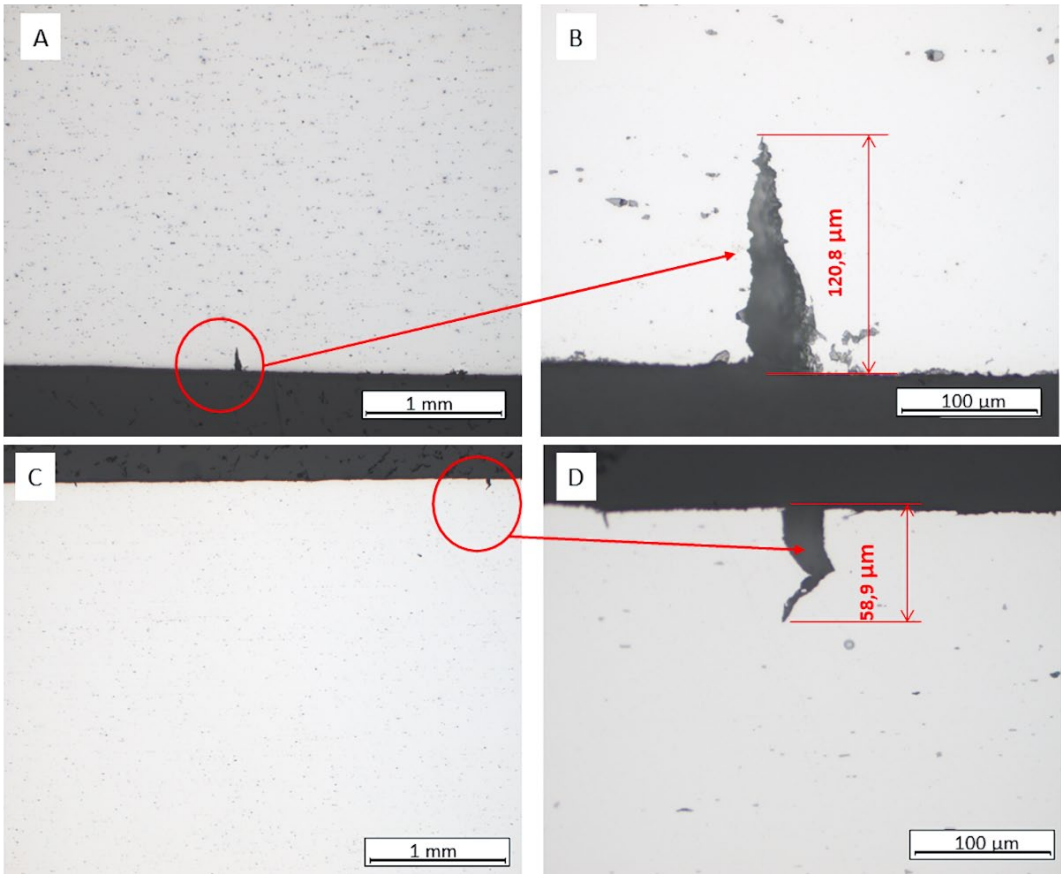

Fig. 8. Microstructure of the EN-AW 7021 alloy, samples a) and b) A1/16 and c) and d) B1/24 of the given SCC with a visible pit at a and c) ×50, and b) and d) ×500

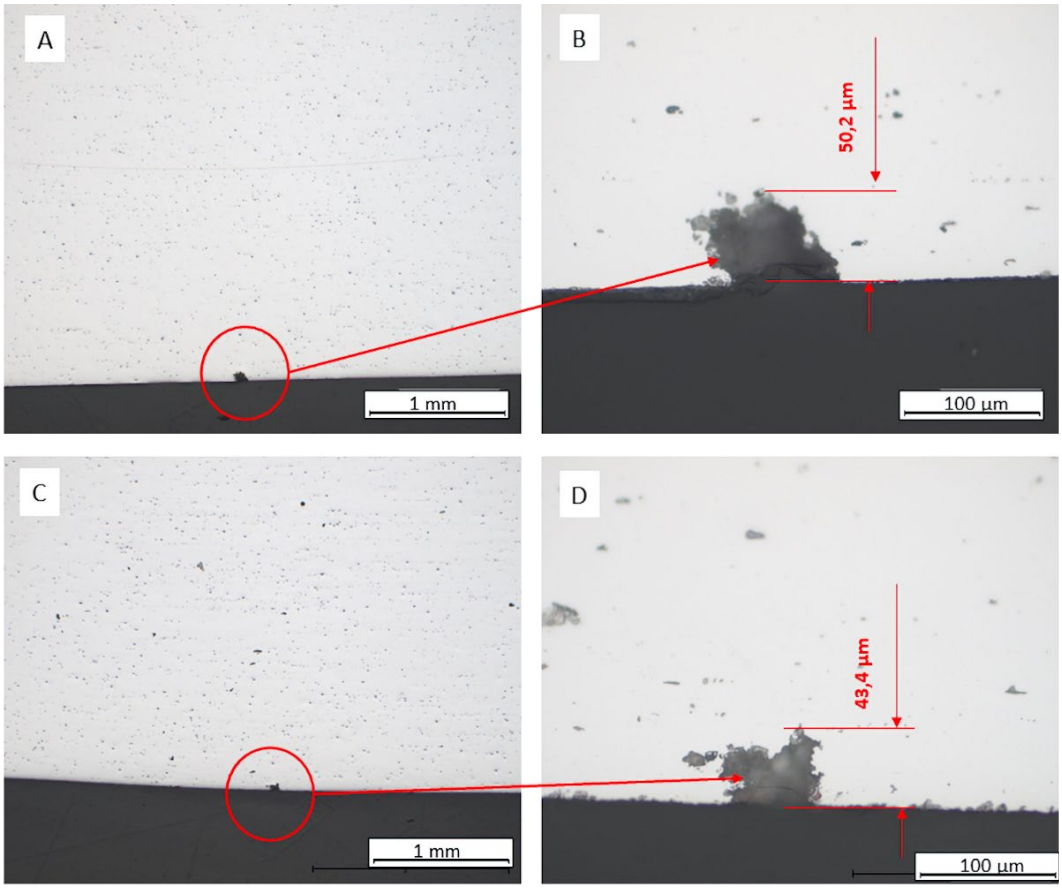

Fig. 9. Microstructure of the EN-AW 7021 alloy, samples a) and b) A1/24 and c) and d) B1/16 of the given corrosion with visible pitting, magnified a and c) ×50, and b) and d) ×500

in Fig. 9 were characteristic of typical corrosion. The stress cracking pits observed on samples A1/16 and B1/24 (Fig. 8) were narrow and elongated towards the inside of the sample.

The pit observed in sample A1/16 was about 120 mm long. On the other hand, the pits in selected samples A1/24 and B/16 (Fig. 9) subjected to stress-free corrosion were small spherical in shape, and the corrosion propagation ran in all directions in the material. The depth of these pits did not exceed 50 mm.

4. Discussion

The EN AW-7021 alloy, in the form of a flat bar subjected to artificial aging in various conditions, achieves strength above 520 MPa. However, these are not the highest values for 7xxx alloys. Alloys obtain higher values after T6 treatment and with the addition of Cu [14,15].

Differences in strength properties were observed between the four selected flat bars. Samples after two-stage treatment had the highest strength properties. Interestingly, the B1/16 sample showed the lowest yield point and the highest elongation among the tested samples. In this TEM sample, a high density of the η' phase was observed compared to the other samples.

These results are consistent with the theory of solid solution [11] and the longer time required to separate high density GP zones resulting in higher strength properties in the case of two-stage aging [16,17]. The analyzes show that the transition time from the GP zones to the η' zones for the B1/16 sample was sufficient to precipitate a high density of the strengthening η' phase. A possible part of these phases has not been transformed from the GP zones to the η' phase, which would indicate the lowest yield point for this sample.

Although the differences in strength properties between the four selected flat bars with different aging parameters were minor and ranged up to a few percent or within the measurement error, corrosion and stress corrosion in them proceed differently. In the samples that were aged in one stage for 16 h (sample A1/16) and in two stages for 24 h (sample B1/24), stress corrosion was found. Largely, the appearance of intergranular corrosion in alloy 7021 was influenced by the extrusion process, supersaturation on the press rundown, and artificial aging. In the sample after one-stage aging 135°C/16 h (A1/16) only finely dispersed phases η' were observed, while in the sample after two-stage aging 90/8 h + 135°C/16 h (B1/16) apart η' phase, $MgZn_2$ precipitates were found inside the grains. Insufficient artificial aging time for the first sample, and thus incomplete disintegration of the solid solution, resulted in a deterioration of the resistance to pitting corrosion. The second sample, in which two-stage aging was applied and the time was the longest, areas with a high concentration of $MgZn_2$ precipitates were observed. Densely distributed precipitates along the grain boundaries, in some places, could have contributed to the poorer resistance to

SCC of the flat bar. Interestingly, in this sample the beginning of intergranular corrosion was found, while in the A1/16 sample only pitting corrosion to the inside of the sample with a length of about 120 mm occurred. According to the standard [12], samples of this type are classified into the 2nd class of resistance to SCC. Resistance class 1 includes flat bars aged in one stage 135°C/24 h (A1/24) and in two stages 90/8 h + 135°C/16 h (B1/16) due to the fact that they did not show defects after SCC. The tests carried out show that the conditions of the aging process for these samples (extended aging process in the case of one-stage aging up to 24 h and a shorter two-stage aging process 8 h + 16 h) turned out to be the most optimal because they achieved high strength properties and resistance to SSC. Both shorter and longer aging time could contribute, on the one hand, to failure to achieve a sufficient density of finely dispersed phases, and to overageing processes where there is an excess of phases, which may lead to easier initiation of cracks in the material during SSC tests [4,11].

The LM observations show that all tested samples showed mild pitting corrosion on the surface after cyclic immersion in the stress-free reagent. The shape and size of the pits was typical for the samples subjected to corrosion. Its appearance could have resulted from local surface defects. The Zn/Mg ratio and the narrow zone free of precipitates have a great influence on SCC [4]. In the case of the tested flat bar, this ratio was 2.6 a, the zone free of precipitations did not exceed 50 nm. Therefore, it can be concluded that the properly selected parameters of one- and two-stage aging of the EN AW-7021 alloy flat bar contributed to the achievement of high resistance to SCC with equally high strength properties.

5. Conclusions

- Based on the aging curves for single-stage (135 and 160°C) and two-stage (90°C/8 h to 135°C, 90°C/8 h to 160°C) aging, it was found that higher hardening of the work occurs in the lower temperature process.
- The analysis of the microstructure on the TEM shows that in the tested alloys of the EN AW-7021 series, after one-stage and two-stage aging for 16h and 24 h, the solid solution disintegrates and the η' phase is released. After treatment A1/24 and B1/16 and B1/24, in some areas, the expanded $MgZn_2$ phases are visible, non-homogenously distributed, occupying areas of several grains.
- After the aging, a large increase in YS and UTS was found compared to the state after supersaturation. The strength properties for the four tested aging conditions were comparable and amounted to approx. 470 MPa for YS and approx. 520 MPa for UTS. Slight differences were observed in the elongation values, where for two-stage treatments a slightly higher plasticity was found by about 2% than for one-stage treatments. The elongation after supersaturation and after two-stage heat treatments was lower by about 2% on average.
- Stress corrosion tests and microscopic observations of the EN AW-7021 alloy showed the highest resistance to SCC for the variants of applied heat treatment – aging at 135°C for 24 h (sample A1/24) and two-stage aging for 16 h (sample B1/16). The remaining variants showed slightly lower resistance to SCC due to the appearance of small pitting observed at ×50 magnification.

Acknowledgments

This research was funded by THE NATIONAL CENTRE FOR RESAERCH AND DEVELOPMENT, grant number TECHMATSTRATEG2/406439/10/NCBR/2019 “Extrusion welding of high-strength sections from 7XXX series aluminium alloys”.

The authors thank Mr. Henryk Jurczak and his colleagues from the Albatros Alumnium company for their help in the implementation of works related to the extrusion process of the 7021 alloy.

REFERENCES

[1] J. Oñoro, The stress corrosion cracking behaviour of heat-treated Al–Zn–Mg–Cu alloy in modified salt spray fog testing. Materials and Corrosion **61** (2), 125-129 (2010). DOI: https://doi.org/10.1002/maco.200905255

[2] L.K Berg., J. Gjønnes, V. Hansen, X.Z. Li, M. Knutson-Wedel, G. Waterloo, D. Schryvers, L.R. Wallenberg. GP-zones in Al–Zn–Mg alloys and their role in artificial aging. Acta Mater. **49**, 3443-3451 (2001). DOI: https://doi.org/10.1016/S1359-6454(01)00251-8

[3] M. Liu, B. Klobes, K. Maier, On the age-hardening of an Al–Zn–Mg–Cu alloy: A vacancy perspective. Scr. Mater. **64**, 21-24 (2011). DOI: https://doi.org/10.1016/j.scriptamat.2010.08.054

[4] Y. Dai, L. Yan, Jianpeng Hao, Review on Micro-Alloying and Preparation Method of 7xxx Series Aluminum Alloys: Progresses and Prospects; Materials **15,** 1216 (2022). DOI: https://doi.org/10.3390/ma15031216

[5] Z. Shan , S. Liu, L. Ye, Y. Li, C. He, J. Chen, J. Tang, Y. Deng, X. Zhang, Article Mechanism of Precipitate Microstructure Affecting Fatigue Behavior of 7020 Aluminum Alloy. Materials **13**, 3248 (2020). DOI: https://doi.org/10.3390/ma13153248

[6] C. Umamaheshwer Rao, V. Vasu, M. Govindaraju, K.V. Sai Srinadh, Stress corrosion cracking behaviour of 7xxx aluminum alloys: A literature review. Trans. Nonferrous Met. Soc. China **26**, 1447-1471 (2016). DOI: https://doi.org/10.1016/S1003-6326(16)64220-6

[7] M. Sirois, M. Bouchard, A. Raude, R. Boba, Stress corrosion – when the defect depth is important, Non Destructive Testing and Diagnostics **3**, 43-46 (2017).

[8] A. Kowalski, W. Ozgowicz, W. Jurczak, A. Grajcar, S. Boczkal, J. Żelechowski, Microstructure, Mechanical Properties, and Corrosion Resistance of Thermomechanically Processed AlZn6Mg0.8Zr Alloy; Materials **11**, (4), 570 (2018). DOI: https://doi.org/10.3390/ma11040570

[9] Cao Xinyu, Zhang Yingbo, Li Jiaheng, Chen Hui, Composition design of 7XXX aluminum alloys optimizing stress corrosion cracking resistance using machine learning, Mater. Res. Express **7**, 046506 (2020).
DOI: https://doi.org/10.1088/2053-1591/ab8492

[10] M. Chemingui, M. Khitouni, K. Jozwiak, G. Mesmacque, A. Kolsi, Characterization of the mechanical properties changes in an Al–Zn–Mg alloy after a two-step ageing treatment at 70° and 135°C. Materials and Design **31**, 3134-3139 (2010).
DOI: https://doi.org/10.1016/j.matdes.2009.12.033

[11] ASM Handbook, Heat Treating of Aluminum Alloys **4**, 841-879 (1991). DOI: https://doi.org/10.1361.asmhba0001205

[12] ECSS-Q-ST-70-37C, Space product assurance – Determination of the susceptibility of metals to stress-corrosion cracking, 15 (2008).

[13] PN-EN ISO 6892-1, Standard Europe. Metallic material – Tensile testing – Part 1: Method of test at room temperature (2019).

[14] S. Sajadifar, P. Krooß, H. Fröck, B. Milkereit, O. Kessler, T. Niendorf. Effects of Aging under Stress on Mechanical Properties and Microstructure of EN AW 7075 Alloy. Metals **11**, 1142 (2021).
DOI: https://doi.org/10.3390/met11071142

[15] Z. Zhao, R. Wu, B. Wang, M. Huang, G. Lei, F. Luo, Effects of Aging on the Microstructure and Properties of 7075 Al Sheets. Materials **13** (18), 4022 (2020).
DOI: https://doi.org/10.3390/ma13184022

[16] M. Orłowska, E. Ura-Binczyk, L. Snieezek, P. Skudniewski, M. Kulczyk, B. Adamczyk-Cieslak, K. Majchrowicz; The Influence of Heat Treatment on the Mechanical Properties and Corrosion Resistance of the Ultrafine-Grained AA7075 Obtained by Hy drostatic Extrusion. Materials **15**, 12 (2022).
DOI: https://doi.org/10.3390/ma15124343

[17] P. Zhou, Y. Song, J. Lu, L. Hua, W. Wu, Q. Sun, J. Su, Novel fast-aging process for Al–Zn–Mg–Cu alloy sheets and its micromechanisms. Materials Science and Engineering A **856**, 20 (2022).